IOP Publishing Measurement Science and Technology
Meas. Sci. Technol. **26** (2015) 085020 (9pp) doi:10.1088/0957-0233/26/8/085020

Performance enhancement for GPS positioning using constrained Kalman filtering

Fei Guo, Xiaohong Zhang and Fuhong Wang

School of Geodesy and Geomatics, Wuhan University, 129 Luoyu Road, Wuhan 430079, People's Republic of China

E-mail: fguo@sgg.whu.edu.cn, xhzhang@sgg.whu.edu.cn and fhwang@sgg.whu.edu.cn

Received 11 November 2014, revised 26 March 2015
Accepted for publication 24 April 2015
Published 16 July 2015

Abstract

Over the past decades Kalman filtering (KF) algorithms have been extensively investigated and applied in the area of kinematic positioning. In the application of KF in kinematic precise point positioning (PPP), it is often the case where some known functional or theoretical relations exist among the unknown state parameters, which can be and should be made use of to enhance the performance of kinematic PPP, especially in an urban and forest environment. The central task of this paper is to effectively blend the commonly used GNSS data and internal/external additional constrained information to generate an optimal PPP solution. This paper first investigates the basic algorithm of constrained Kalman filtering. Then two types of PPP model with speed constraints and trajectory constraints, respectively, are proposed. Further validation tests based on a variety of situations show that the positioning performances (positioning accuracy, reliability and continuity) from the constrained Kalman filter are significantly superior to those from the conventional Kalman filter, particularly under extremely poor observation conditions.

Keywords: GPS, precise point positioning, Kalman filter, speed constraints, trajectory constraints

(Some figures may appear in colour only in the online journal)

1. Introduction

Positioning with GNSS (such as GPS, GLONASS and BDS, etc.) can be performed by either point positioning or relative positioning. Surveying with GNSS has conventionally been carried out in the differential positioning model, mainly due to the higher potential positioning accuracy compared to that of the standard point positioning (SPP). However, the point positioning technique is much easier and has lower operational cost than the relative positioning technique. This makes point positioning an attractive method for low-cost GNSS applications. To achieve the highest possible GNSS point positioning accuracy, dual-frequency carrier phase and pseudo-range measurements are utilized simultaneously, and precise satellite ephemeris and clock errors are provided. In addition, all the remaining un-modeled errors due to satellite antenna phase offsets, satellite orientation, tropospheric delay, and various site displacement effects such as Earth tide and ocean loading must be addressed. This approach is commonly known as precise point positioning (PPP). Recent studies show that PPP is free from the constraints of baseline lengths, and the accuracy of PPP is comparable to that of relative positioning, suggesting an efficient and cost-effective solution for highly precise kinematic positioning for land/marine/space platforms (e.g. Zhang and Andersen 2006, Geng *et al* 2010).

PPP technology can provide centimeter to decimeter, or even millimeter-level positioning accuracy under 'clear sky' conditions using a Kalman filter (KF), which is regarded as an optimal estimator (Kalman 1960, Gelb 1974). However, the optimality of the estimation is closely connected to the quality of the prior information about the process noise and the updated mesurement noise, which are sometimes difficult

to obtain (e.g. Yang *et al* 2001, Hide *et al* 2003, Ding *et al* 2007, Almagbile *et al* 2010). In addition, topographic and biological obstacles tend to degrade PPP positioning performance and can even cause failure of the PPP solution, particularly in urban and forest areas (Erik *et al* 2008, Ahmed *et al* 2012). Working in an obstacle environment the user will typically view only a few satellites that are high overhead. As satellites are clustered together, this results in poor GDOP (geometric dilution of precision), which has a large detrimental effect on the accuracy of PPP solution. Moreover, the view of the sky may change rapidly and frequently, especially when the target is moving with high maneuvering. This may cause inevitable data discontinuity due to cycle slips, data gaps and loss-of-lock, and consequently degrades the accuracy and continuity of the PPP solution (Zhang *et al* 2011). In order to enhance PPP performance, several schemes such as robust Kalman filtering and adaptive Kalman filtering have been proposed to resist observational errors and unexpected state turbulence (e.g. Guo and Zhang 2014). On the other hand, augmented algorithms that make use of the satellite- or ground-based information have been developed to bridge the observation discontinuities (Geng *et al* 2010, Li *et al* 2011). Although the effectiveness of these algorithms has been demonstrated, the efficiency and cost are still problematic challenges for general users.

In the application of KF in kinematic PPP, it is often the case where some known functional or theoretical relations exist among the unknown state parameters, which can be made use of to improve the accuracy and reliability of the state estimates (Yang *et al* 2010). For example, the Doppler or derived Doppler observations can be used to strengthen the structure of the measurement space. The approximate traveling direction or route is known and can be used to bind its trajectory. Moreover, the outputs from external sensors like speedometer, accelerometer and INS in general can be taken into account for the improvement of PPP performance. This paper aims at introducing the constrained Kalman filtering to enhance PPP performance. First, two filters with velocity constraints and trajectory constraints are designed for PPP, and then the kinematic PPP performances are compared with that of conventional Kalman filtering.

2. Constrained Kalman filtering

2.1. Basic model

The well-known Kalman filter (KF) is a powerful tool in the analysis of dynamic systems. The filter operates recursively on streams of noisy input data to produce a statistically optimal (minimum mean square error) estimate of the underlying system states, and has been extensively applied in the fields of engineering such as control theory, communication systems, satellite navigation and aerospace applications.

Considering a state sequence $\{X_k, k = 0, 1, 2, \cdots, n\}$ and observations $\{L_k, k = 0, 1, 2, \cdots, n\}$ whose time evolution and observation equations are described by the following linear model (Kalman 1960, Gelb 1974):

$$\begin{cases} X_{k+1} = \Phi_{k+1,k} X_k + \Gamma_k w_k \\ L_k = H_k X_k + v_k \end{cases} \tag{1}$$

where $X_k \in \Re^n$ is state vector, $L_k \in \Re^m$ is measurement vector, $\Phi_{k+1,k}$ is state transition matrix, H_k is observation (design) matrix and Γ_k is noise matrix. w_k and v_k are respectively the process noise and measurement noise vector, which are assumed to be uncorrelated Gaussian white noise with zero mean and covariance Q_k and R_k:

$$\mathrm{E}[w_k w_i^{\mathrm{T}}] = \begin{cases} Q_k & i = k \\ 0 & i \neq k \end{cases}; \ \mathrm{E}[v_k v_i^{\mathrm{T}}] = \begin{cases} R_k & i = k \\ 0 & i \neq k \end{cases}; \ \mathrm{E}[w_k v_i^{\mathrm{T}}] = 0 \text{ for all } i \text{ and } k \tag{2}$$

where $\mathrm{E}[\cdot]$ denotes expectation, and superscript 'T' represents matrix transpose.

Compared with the basic model of conventional KF as shown in equations (1) and (2), the constrained KF introduces some state constraints. The linearized constraints equations can be generally expressed as:

$$D_k \cdot X_k - d_k = 0 \tag{3}$$

where D_k is a design matrix with rank r_k (the number of constraints equation), d_k is a constant vector composed of some fixed values.

2.2. Recursive estimator with constraints

In general, there are three approaches to dealing with the prior constraints in Kalman filtering. The first approach is to reduce the state parameters using the state constraints, and then perform a standard Kalman filtering without constraints. The second way is to transform the constraints as measurement equations which strengthen the structure of the measurement space directly. The third method is to solve a Lagrangian equation with the consideration of the state constraints, which project the state estimate onto the constraint surface (Simon 2010). In fact, the above three approaches dealing with the state constraints are equivalent (Yang *et al* 2010). To easily understand the contribution of the state constraints on the state estimates and their corresponding covariance matrix of the filtering, the third approach is employed to derive the recursive algorithm for the constrained Kalman filter.

The KF is a minimum mean-square error (MMSE) estimator. Therefore, the criterion for constrained Kalman filtering is to minimize the following cost function:

$$\begin{cases} \mathrm{E}(\|X - X'\|^2 | L) = \min \\ D \cdot X' = d \end{cases} \tag{4}$$

where X' denotes the estimates with constraints. The optimal solution can then be obtained by solving a Lagrangian equation.

For the sake of simplicity, the recursive equations of the constrained KF take the following general form (Liu *et al* 2008):

$$\hat{X}_{k,k-1} = \Phi_{k,k-1} \hat{X}_{k-1} \tag{5}$$

$$P_{k,k-1} = \Phi_{k,k-1} P_{k-1} \Phi^{\mathrm{T}}{}_{k,k-1} + \Gamma_{k-1} Q_{k-1} \Gamma^{\mathrm{T}}{}_{k-1} \quad (6)$$

$$X'_{k,k-1} = \hat{X}_{k,k-1} - D_k^{\mathrm{T}} (D_k D_k^{\mathrm{T}})^{-1} (D_k \hat{X}_{k,k-1} - d_k) \quad (7)$$

$$P'_{k,k-1} = [I - D^{\mathrm{T}} (DD^{\mathrm{T}})^{-1} D]^{\mathrm{T}} P_{k,k-1} [I - D^{\mathrm{T}} (DD^{\mathrm{T}})^{-1} D] \quad (8)$$

$$K_k = P'_{k,k-1} H_k^{\mathrm{T}} (H_k P'_{k,k-1} H_k^{\mathrm{T}} + R_k)^{-1} \quad (9)$$

$$\hat{X}_k = X'_{k,k-1} + K_k (L_k - H_K X'_{k,k-1}) \quad (10)$$

$$P_k = (I - K_k H_k) P'_{k,k-1} (I - K_k H_k)^{\mathrm{T}} + K_k R_k K_k^{\mathrm{T}} \quad (11)$$

Where $\hat{X}_{k,k-1}$ and $P_{k,k-1}$ represent the predicted state vector and its covariance matrix without constraint, $X'_{k,k-1}$ and $P'_{k,k-1}$ denote the corrected predicted state vector and its covariance matrix by constrained equations, $\hat{X}_k$ and P_k are respectively the final estimated state and its covariance matrix, K_k is the filter gain matrix, which defines the updating weight between new measurements and predictions from the system dynamic model and I is an identity matrix.

It is easily observed that the recursive form of the constrained KF is consistent with the conventional KF. Only the predicted state vector and its covariance matrix are corrected by constrained equations. It should be noted that (5)–(11) show the general recursive algorithm. Actually, once the (robust) equivalent covariance and adaptive factor are adopted, the above model can be further extended to be the adaptive robust KF with constraints.

3. PPP model with constrained equations

3.1. State-space model

To be able to apply the KF for PPP, one should first construct a state-space model, which is represented by two equations: one describes the explicit relation between observations and unknowns (observation model), and the other one describes the evolution of the parameters (dynamic model). In this paper, the most popular ionosphere-free combinations of dual-frequency code and carrier phase observations are used to form the PPP observation model. For the sake of simplicity, the observation model is illustrated in the following equations:

$$P_{\mathrm{IF}} = \frac{f_1^2}{f_1^2 - f_2^2} P_1 - \frac{f_2^2}{f_1^2 - f_2^2} P_2$$
$$= \rho + c \cdot dt + d_{\mathrm{trop}} + d^s_{\mathrm{hd}(P(L_1,L_2))} - d_{r(\mathrm{hd}(P(L_1,L_2)))} + d_{\mathrm{mult}(P(L_1,L_2))} + \varepsilon_{P(L_1,L_2)} \quad (12)$$

$$\Phi_{\mathrm{IF}} = \frac{f_1^2}{f_1^2 - f_2^2} \Phi_1 - \frac{f_2^2}{f_1^2 - f_2^2} \Phi_2$$
$$= \rho + c \cdot dt + d_{\mathrm{trop}} + N_{\mathrm{IF}} + B_{\mathrm{IF}} + d^s_{\mathrm{hd}(\Phi(L_1,L_2))} - d_{r(\mathrm{hd}(\Phi(L_1,L_2)))} + d_{\mathrm{mult}(\Phi(L_1,L_2))} + \varepsilon_{\Phi(L_1,L_2)} \quad (13)$$

where P_{IF} is the ionosphere-free combinations of P_1 and P_2 pseudo-ranges, Φ_{IF} is the ionosphere-free combinations of Φ_1 and Φ_2 carrier phases (in units of distance), ρ is the true geometry range, c is the speed of light in vacuum, dt is receiver clock error, d_{trop} is tropospheric delay, $d^s_{\mathrm{hd}(\cdot)}$ and $d_{r(\mathrm{hd}(\cdot))}$ is the satellite and receiver hardware bias, respectively, N_{IF} is the integer phase ambiguity of the ionosphere-free phase combination, B_{IF} is the initial phase of the satellite oscillator, $d_{\mathrm{mult}(\cdot)}$ and ε are the combined multipath effect and measurement noise. To achieve an accurate and reliable solution from PPP, effects such as sagnac, tide errors, carrier phase wind-up and transmitter antenna phase offset must be corrected using models. Interested readers can refer to, e.g. Zumberge *et al* (1997) and Kouba *et al* (2001) for a full parameterization discussion.

As to the dynamic model, the constant-acceleration (CA) model assuming an object moving with a fixed acceleration is employed for state transition. The following equations show the simplified dynamic model:

$$X_{\mathrm{state}} = \begin{bmatrix} X_{\mathrm{pos}} \\ X_{\mathrm{vel}} \\ X_{\mathrm{acc}} \end{bmatrix}_k = \begin{bmatrix} I_{3\times3} & \Delta t \cdot I_{3\times3} & \Delta t^2/2 \cdot I_{3\times3} \\ 0_{3\times3} & I_{3\times3} & \Delta t \cdot I_{3\times3} \\ 0_{3\times3} & 0_{3\times3} & I_{3\times3} \end{bmatrix} \begin{bmatrix} X_{\mathrm{pos}} \\ X_{\mathrm{vel}} \\ X_{\mathrm{acc}} \end{bmatrix}_{k-1} + \begin{bmatrix} 0_{3\times3} \\ 0_{3\times3} \\ I_{3\times3} \end{bmatrix} w_{\mathrm{state}}(k) \quad (14)$$

where X_{pos}, X_{vel} and X_{acc} respectively refers to the state of position, velocity and acceleration, Δt denotes sampling interval.

3.2. PPP with speed constraints

The pseudo-range and carrier phase are the two fundamental types of observables for GNSS. In fact, Doppler observations can be simultaneously produced by several GNSS receivers or derived from carrier phases. These original or derived Doppler observations are considered helpful for velocity determination. Furthermore, some prior state information from external sensors such as speedometer and accelerometers, which will not be affected by the real observing environment and sensitive to the state disturbance, are available and hence valuable for enhancing the robustness of PPP.

As shown in the above sections, a critical issue for PPP solution with constrained KF lies in the design of constrained equations. Therefore, the basic methodology and algorithm of PPP with speed constraints are not repeated, only the constrained condition is given according to the following equations:

$$D \cdot X_{\mathrm{state}} - d = 0 \quad (15)$$

where

$$D = \begin{bmatrix} 0 & 0 & 0 & 1 & 0 & 0 & 0 & 0 & 0 \\ 0 & 0 & 0 & 0 & 1 & 0 & 0 & 0 & 0 \\ 0 & 0 & 0 & 0 & 0 & 1 & 0 & 0 & 0 \end{bmatrix} \quad (16)$$

and

$$d = [vel_x \quad vel_y \quad vel_z]^{\mathrm{T}} \quad (17)$$

vel_x, vel_y and vel_z are the prior velocities of three different components, which can be estimated from Doppler observations

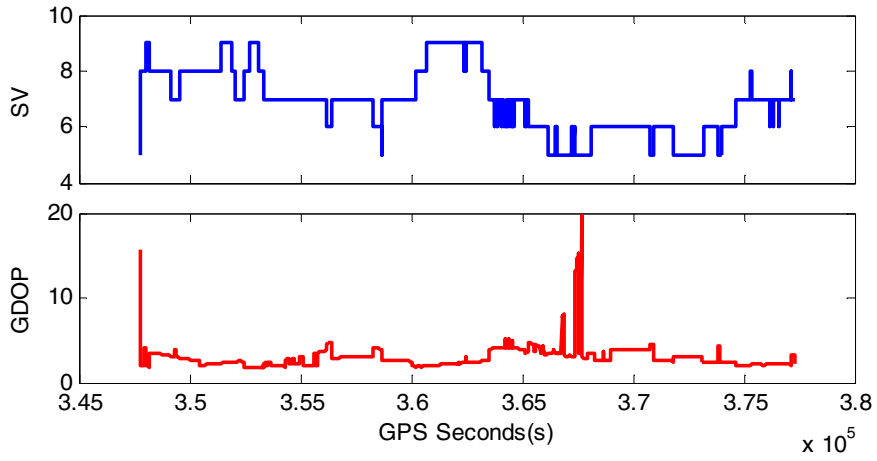

Figure 1. The number of visible satellites (SV) and geometric dilution of positioning (GDOP) at a static site located in Wuhan district.

or read directly from external sensors. Once the design matrix D and constant vector d are obtained, the states of the system at any time can be recursively estimated by (5)–(11).

3.3. PPP with trajectory constraints

For a moving object, there can be some underlying constraints which may be used to enhance PPP solution. For example, a car/ship/aircraft always moving along its route and its trajectory should not deviate from the road/route itself. In this case, most of the road/route can be abstracted as a series of straight line equations (Zuo *et al* 2004, Chen *et al* 2012).

Let the road linear equation be defined as:

$$N = \alpha \cdot E + m \tag{18}$$

where N and E represent the north and east components in a 2D horizontal coordinate system, α and m denotes the azimuth and intercept of the road linear equation, respectively.

Considering the moving direction remains unchanged in a certain time interval, the following equations can be listed to constrain the vehicle's trajectory:

$$\begin{cases} S_N = \alpha \cdot S_E + m \\ V_N = \alpha \cdot V_E \end{cases} \tag{19}$$

where S_N and S_E are coordinates of the north and east components, V_N and V_E are velocities of the north and east components. In addition, expression (19) can be written as:

$$D \cdot X_{\text{state}} - d = 0 \tag{20}$$

where

$$D = \begin{bmatrix} -\alpha & 0 & 0 & 1 & 0 & 0 & 0 & 0 & 0 \\ 0 & -\alpha & 0 & 0 & 1 & 0 & 0 & 0 & 0 \end{bmatrix} \tag{21}$$

and

$$d = [m \quad 0]^{\mathrm{T}} \tag{22}$$

X_{state} is the estimated states in a Topocentric-horizon coordinate system. Similarly, given the constraint matrix D and constant vector d, we can easily calculate the unknowns according to (5)–(11).

4. Experimental results and analysis

In this section, PPP solutions in simulated and real kinematic scenes are provided to illustrate the performance of constrained KF algorithm. Static state can be regarded as a special case of kinematic state with exactly known and fixed prior information, such as speed, acceleration, direction angle, etc. Therefore, simulated kinematic PPP using static observations is the most direct and effective validation of the constrained KF. Also, a car-borne kinematic PPP experiment was carried out to test its effectiveness in a real world situation with high dynamics and complex motion. Products such as precise satellite orbit, clock error, and differential code bias required for PPP were provided by the community of international GNSS service.

4.1. PPP solutions with speed constraints

4.1.1. Case 1: simulated kinematic PPP. To validate the contribution of speed constraints to kinematic PPP, a set of static GPS observation recorded on November 20, 2008 (UTC 00:30–08:30, 1 s sampling interval), in Wuhan district were used for epoch-wise PPP solution. The number of visible satellite vehicles (SV) and geometric dilution of positioning (GDOP) during the observed time are plotted in figure 1. Experimental studies were performed with the following two filtering schemes:

Scheme 1: Conventional Kalman filtering (KF) without speed constraints.

Scheme 2: Constrained Kalman filtering (CKF) with speed constraints (set vehicle velocity and acceleration to zero).

The corresponding positioning results were obtained, and the differences with respect to the known coordinates are presented in figure 2.

It can be observed that both schemes reach a few decimeters or even centimeter positioning accuracy after a short convergence. However, large variations up to one meter can be observed during the periods 05:23–06:46 UT ($3.65–3.7 \times 10^5$ GPS seconds) when the conventional KF was adopted for epoch-wise PPP solution. This is reasonable

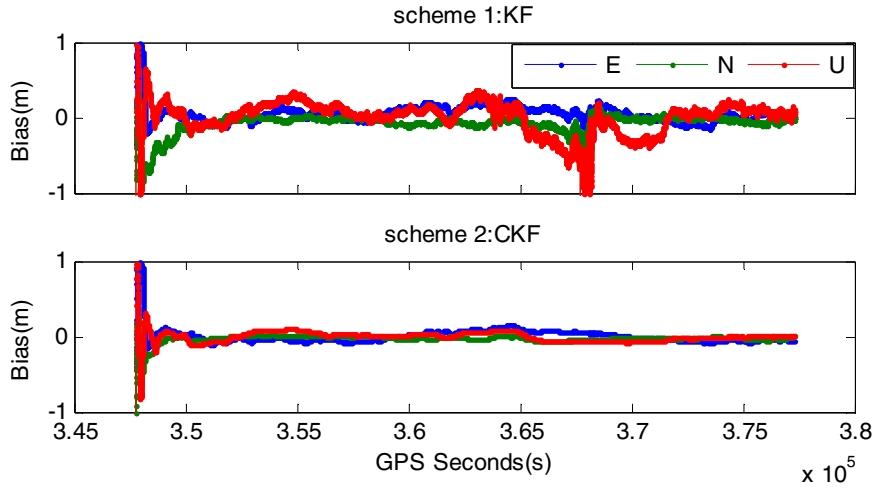

Figure 2. Error series of the estimated coordinates in the east (E), north (N) and up (U) components. The upper one shows the results of scheme 1 (KF), and the lower one shows the results of scheme 2 (CKF).

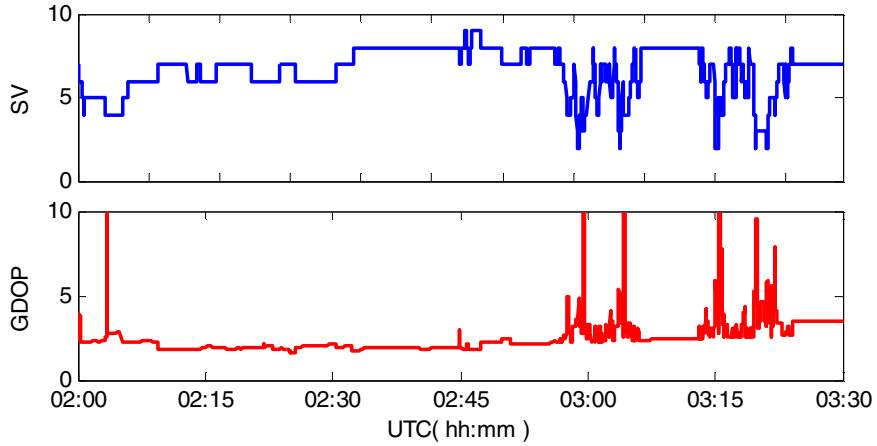

Figure 3. The number of visible satellites (SV) and geometric dilution of positioning (GDOP) for the car-borne GPS data.

taking into account that the available satellites decrease and the GDOP increases dramatically during this period as shown in figure 1. Once the constrained KF is applied, we can get smoothly running and precise coordinate solutions even under the presence of extremely poor observation condition. Due to the prior speed constrained information, it significantly improves the positioning accuracy and reliability of kinematic PPP.

4.1.2. Case 2: car-borne kinematic PPP. Further validation was performed for real kinematic data. A typical example using a set of car-borne GPS data generated at 1 s intervals for 1.5 h (UT 02:00–03:30) is presented and analyzed in this section. The car drove repeatedly around a ring road, and the SV and GDOP are shown in figure 3.

The following three schemes were designed for kinematic PPP solution:

Scheme 1: conventional KF without constraints; and the states of position, velocity and acceleration are modeled as white noises (KF + WN).

Scheme 2: conventional KF without constraints; and a constant acceleration (CA) process is used for the dynamic model (KF + CA).

Scheme 3: constrained KF using prior speed information from Doppler observations; and a constant acceleration (CA) process is used for the dynamic model (CKF + CA).

The positioning results obtained from the above three PPP filters are compared in figure 4, in which the upper three plots show the estimated vehicle trajectory and the lower three plots show the uncertainties of the position. The horizontal and vertical axes of the upper three plots represent the east and north components (in units of meters), respectively. For the lower three plots, the horizontal axes represent observing time (UT: hour/minute), while the vertical axes denote the standard error of position estimates in a 3D topocentric coordinate system (in units of meters).

As illustrated in figure 3, the number of available satellites decreases to 2–4 and its corresponding GDOP increases over 10 several times. The reason for this may be attributed to signals being blocked by viaducts or high-rise buildings in the city. During these periods, the positioning accuracy as shown in figure 4 decreases dramatically, particularly for the first scheme which suffers from insufficient observations. Consequently, the vehicle trajectory wanders significantly from the path, or even fails to be located. Compared with the first scheme, a more precise dynamic model is provided

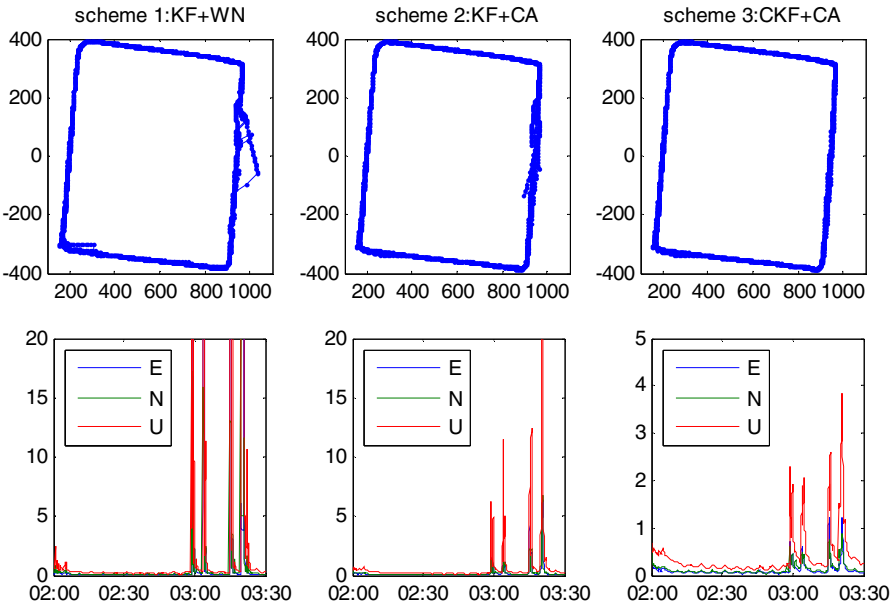

Figure 4. Estimated positions and their precisions (1 sigma) with three different schemes. The upper plots show the horizontal trajectory of the vehicle, and the lower ones show the standard deviations of positioning estimates.

in scheme 2, and the estimated state can be transmitted by a constant acceleration model, even in the case of an insufficient number of satellites. Obviously, the positioning results of scheme 2 are improved to some extent. But path deviations can still be observed from its trajectory. Once an explicit dynamic model and speed constraints are applied in scheme 3, the filter significantly enhances the kinematic PPP performance. The vehicle trajectory is much smoother than with the other two schemes, and the uncertainty of position estimates is significantly reduced. This is reasonable when we acknowledge the fact that the constraints strongly bound the errors of the state estimates, and the filter gain is sensitive to the certainty of the measurements and current state estimates. With a high gain, the filter places more weight on the measurements, while the filter follows the predictions of the dynamic model more closely with a low gain. At the extremely poor observation conditions (a near-zero gain), the contribution of measurements is reduced or even ignored, while the state estimates are taken full advantage of to keep relatively accurate predictions for a short time.

4.2. PPP solutions with trajectory constraints

4.2.1. Case 1: simulated kinematic PPP. Likewise, the same static GPS data was used to verify the performance of kinematic PPP with trajectory constraints. For a static vehicle, it can be regarded as a moving object with fixed direction. Assuming the direction cosines of the static GPS receiver antenna are (α, β, γ), the following four schemes were performed:

Scheme 1: epoch-wise PPP solution using conventional KF.

Scheme 2: epoch-wise PPP solution using constrained KF with fixed α.

Scheme 3: epoch-wise PPP solution using constrained KF with fixed β.

Scheme 4: epoch-wise PPP solution using constrained KF with fixed γ.

Figures 5 and 6 show the positioning errors and trajectories of the four different schemes. As can be seen in figure 5, the positioning accuracy of the constrained KF with trajectory constraints (scheme 2–4) are obviously superior to that of conventional KF, because the moving directions are bound to fixed values. The reason for the poor performances in the first scheme was explained in section 4.1 and hence will not be discussed.

As shown in figure 6, a discrete and dispersed distribution of the tracking points can be observed in scheme 1, while the other three schemes show regular and centralized trajectories, distributed in approximately straight lines. To some extent, the slope of the straight line reflects the differences in precision between the east–west (EW) and the north–south (NS) directions. For example, the trajectory of scheme 2 runs a near north–south line (with a steep slope close to ± 1), which means the precision of the EW is superior to that of NS. However, the trajectory of scheme 4 shows a near north–south line (with a slope close to 0), which means the precision of the NS is much better than that of EW. In particular, when the tracking route is approximate an east–south line (with a slope close to ± 0.5) as shown in scheme 3, the precision of the EW is comparable to that of NS.

4.2.2. Case 2: car-borne kinematic PPP. Similarly, experimental studies were carried out in real dynamic scenes, and the same car-borne GPS data as described in section 4.1 was used to verify the performance of kinematic PPP with trajectory constraints. As shown in figure 4, the ring road can be abstracted as piecewise straight line equations. For convenience, only a north–south orientation segment was selected to be shown. Kinematic PPP tests were performed according to the following two schemes:

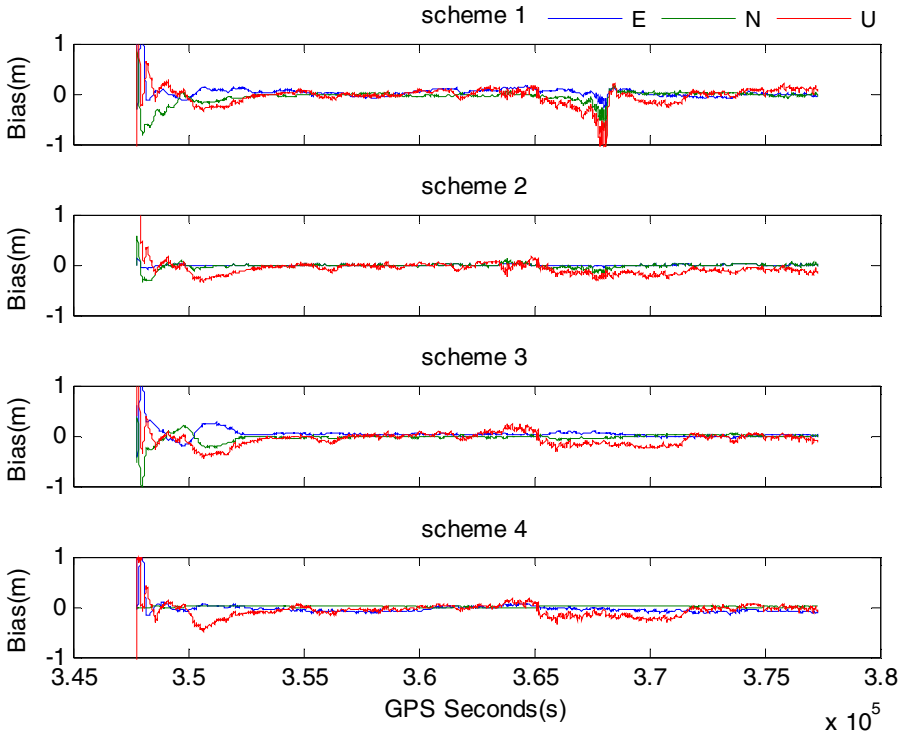

Figure 5. Positoning performances of the four different schemes. The horizontal axes represent GPS time, and the vertical axes represent positioning errors in the east (E), north (N) and up (U) components.

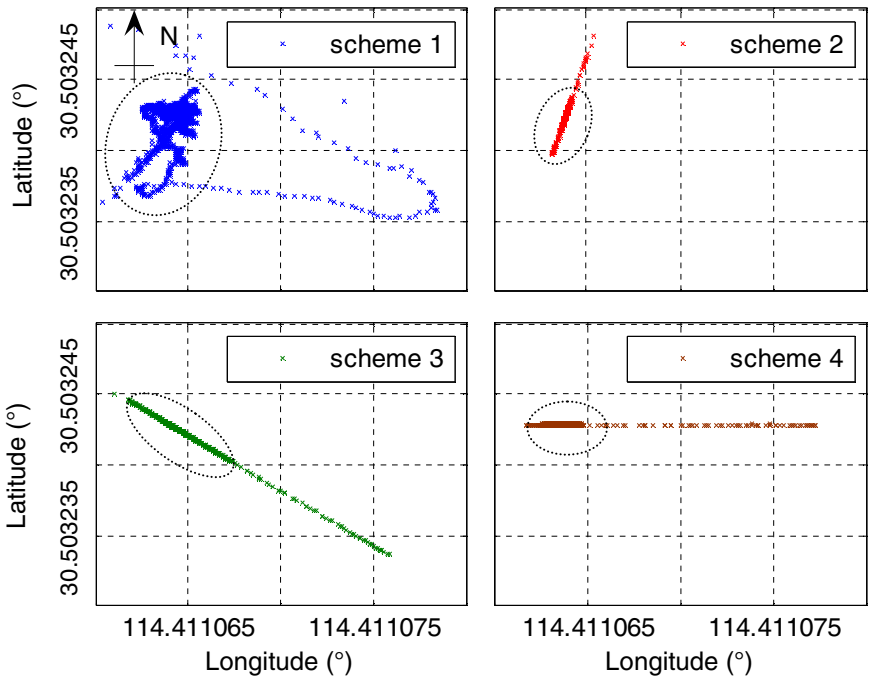

Figure 6. Estimated tracking plots for the four different schemes. The elliptic markings on the graphs show the epoch-wise PPP solution after a short period of convergence.

Scheme 1: conventional KF without any constraint.

Scheme 2: constrained KF with a straight line equation.

The positioning estimates and their precisions are shown in figure 7. The horizontal and vertical axes of the upper two plots represent the east and north components (in units of meters), respectively. In addition, figure 8 shows the estimated velocities of the vehicle using the above two schemes. Due to the extremely poor observation conditions as shown in figure 3, the positioning accuracy of scheme 1 is seriously affected by the sudden reduction of satellites and sharply increased GDOPs. In contrast to the first scheme, a much more continuous and smoother trajectory is obtained, once the constrained KF is applied for kinematic PPP solution (scheme 2). Furthermore, significant improvements can be observed from

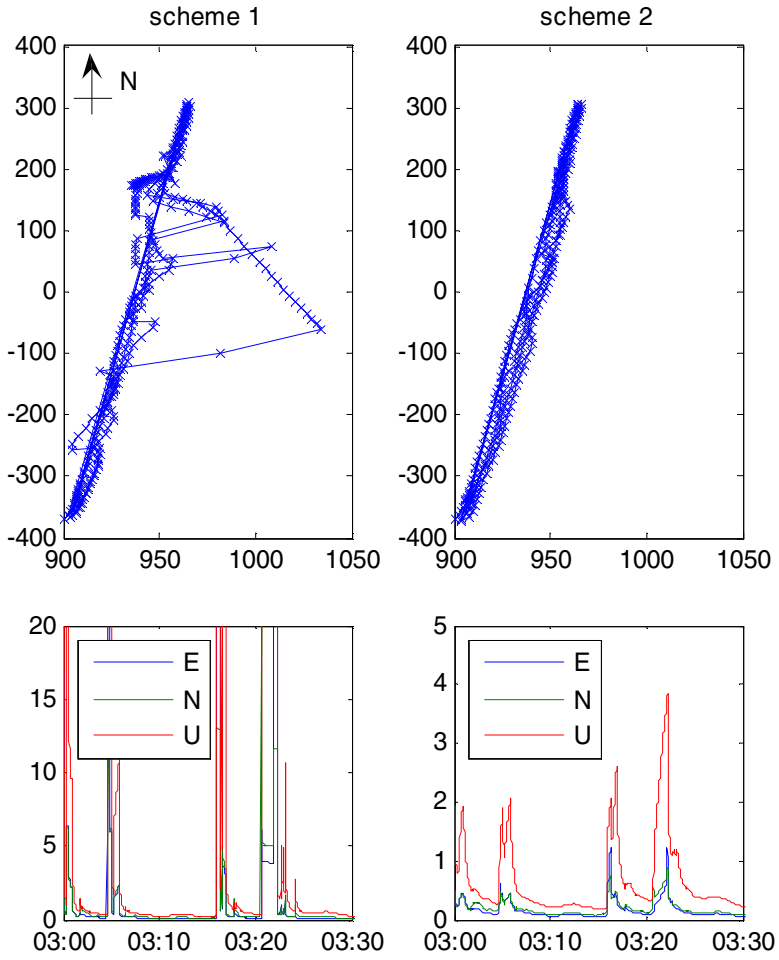

Figure 7. Estimated trajectories and their precisions (1 sigma) with two different schemes. The upper plots show the horizontal tracking points, and the lower ones show the standard deviations of positioning estimates.

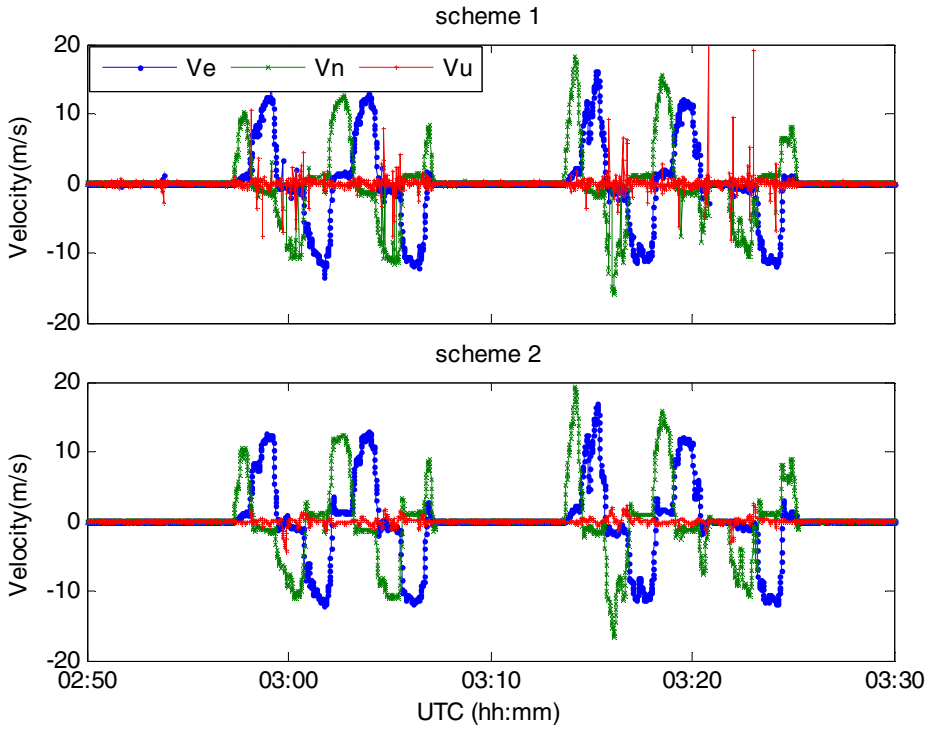

Figure 8. Estimated velocity curves for the two schemes. The upper one shows the vehicle velocities of scheme 1, and the lower one shows the vehicle velocities of scheme 2.

the velocity curves, especially in the vertical direction. The reason for these improvements is obvious, and hence will not be discussed.

It should be noted that the states of a vehicle are inevitably affected by various factors. Sometimes, the tracking plots are not completely consistent with the given constraints. This presents a big challenge for the constraint modeling. In addition, constraint equations should be frequently changed to adapt to the actual situation, and hence it is bound to affect the computational complexity and efficiency. Nevertheless, filters with additional constrained information greatly enhance the kinematic PPP solution under extremely poor observation conditions.

5. Conclusions

Considering some internal or external auxiliary information may be helpful for kinematic positioning, the algorithm of constrained Kalman filtering is applied to enhance the performance of kinematic PPP. We first derive the basic methodology and algorithm of constrained Kalman filtering. Then two models of PPP with speed and trajectory constraints, respectively, are proposed. Tests carried out in a variety of situations, including simulated kinematic PPP and car-borne kinematic PPP have been performed for validation. Numerical results show that the positioning performances of constrained Kalman filter are superior to those of conventional Kalman filter, particularly under extremely poor observation conditions. However, it is worth mentioning that the effectiveness of the constrained Kalman filtering depend on the accuracy of the constraint equations. If the given constraint equations and their covariance are inappropriate, the filter may fail to improve the accuracy and reliability of kinematic PPP, or even cause a failure of convergence. In addition to equality constraints, inequality constraint equations can also be used to enhance the kinematic PPP solution, which needs further study.

Acknowledgments

The authors gratefully acknowledge IGS for providing GNSS products. We also appreciate the handling editor and two anonymous reviewers for their valuable comments and improvements to this manuscript. This study was supported by the National Natural Science Foundation of China (No: 41474025, No: 41404006) and International Postdoctoral Exchange Fellowship Program 2013 by the Office of China Postdoctoral Council (No. 2013042).

References

Ahmed E and Ayman F 2012 Enhancement of GPS single point positioning accuracy using referenced network stations *World Appl. Sci. J.* **18** 1463–74

Almagbile A, Wang J and Ding W 2010 Evaluating the performances of adaptive Kalman filter methods in GPS/INS integration *J. Global Positioning Syst.* **9** 33–40

Chen Z and Liu Q 2012 Application of adaptive velocity constraint filter in excavator GPS system *J. Huaqiao Univ. (Nat. Sci.)* **33** 490–4

Ding W, Wang J and Rizos C 2007 Improving adaptive Kalman estimation in GPS/INS integration *J. Navig.* **60** 517–29

Erik N and Jon G 2008 Performance of GPS point positioning under conifer forest canopies *Photogramm. Eng. Remote Sens.* **74** 661–8

Gelb A 1974 *Applied Optimal Estimation* (Cambridge, MA: MIT)

Geng J, Teferle F N, Meng X and Dodson A H 2010 Kinematic precise point positioning at remote marine platforms *GPS Solut.* **14** 343–50

Guo F and Zhang X 2014 Adaptive robust Kalman filter for kinematic precise point positioning *Meas. Sci. Technol.* **25** 105011

Hide C, Moore T and Smith M 2003 Adaptive Kalman filtering for low cost INS/GPS *J. Navig.* **56** 143–52

Kalman R E 1960 A new approach to linear filtering and prediction problems *Trans. ASME* **82** 35–45

Kouba J and Hérous P 2001 Precise point positioning using IGS orbit and clock products *GPS Solut.* **5** 12–28

Li X, Zhang X and Ge M 2011 Regional reference network augmented precise point positioning for instantaneous ambiguity resolution *J. Geod.* **85** 151–8

Liu Y, Liu J and Zhu D 2008 Application of adaptive Kalman filter restricted by road information to vehicle-borne navigation *Geomatics Inf. Sci. Wuhan Univ.* **33** 828–30

Simon D 2010 Kalman filtering with state constraints: a survey of linear and nonlinear algorithms *IET Control Theory Appl.* **4** 1303–18

Yang Y, Gao W and Zhang X 2010 Robust Kalman filtering with constraints: a case study for integrated navigation *J. Geod.* **84** 373–81

Yang Y, He H and Xu G 2001 Adaptively robust filtering for kinematic geodetic positioning *J. Geod.* **75** 109–16

Zhang X and Li X 2011 Instantaneous re-initialization in real-time kinematic PPP with cycle-slips fixing *GPS Solut.* **16** 315–27

Zhang X H and Andersen O B 2006 Surface ice flow velocity and tide retrieval of the Amery ice shelf using precise point positioning *J. Geod.* **80** 171–6

Zumberge J F, Heflin M B, Jefferson D C, Watkins M M and Webb F H 1997 Precise point positioning for the efficient and robust analysis of GPS data from large networks *J. Geophys. Res.* **102** 5005–17

Zuo J, Bao Y and Liu Y 2004 A new kinematic filtering method with constraint of GPS positioning *Comput. Simul.* **21** 80–3